


Hyperuniformity in the Manna Model, Conserved Directed Percolation and Depinning

Kay Jörg Wiese 

CNRS-Laboratoire de Physique de l'Ecole Normale Supérieure, PSL Research University, Sorbonne Université, Université Paris Cité, 24 rue Lhomond, 75005 Paris, France

 (Received 7 March 2024; revised 28 May 2024; accepted 12 June 2024; published 8 August 2024)

Hyperuniformity is an emergent property, whereby the structure factor of the density n scales as $S(q) \sim q^\alpha$, with $\alpha > 0$. We show that for the conserved directed percolation (CDP) class, to which the Manna model belongs, there is an exact mapping between the density n in CDP, and the interface position u at depinning, $n(x) = n_0 + \nabla^2 u(x)$, where n_0 is the conserved particle density. As a consequence, the hyperuniformity exponent equals $\alpha = 4 - d - 2\zeta$, with ζ the roughness exponent at depinning, and d the dimension. In $d = 1$, $\alpha = 1/2$, while $0.6 > \alpha \geq 0$ for other d . Our results fit well the simulations in the literature, except in $d = 1$, where we perform our own to confirm this result. Such an exact relation between two seemingly different fields is surprising, and paves new paths to think about hyperuniformity and depinning. As corollaries, we get results of unprecedented precision in all dimensions, exact in $d = 1$. This corrects earlier work on hyperuniformity in CDP.

DOI: [10.1103/PhysRevLett.133.067103](https://doi.org/10.1103/PhysRevLett.133.067103)

Context—Hyperuniform (HU) structures have vanishing long-wavelength density fluctuations similar to crystals, but no long-range order [1–3]. The structure factor of the Fourier-transformed particle density, $S_q := \langle n_q n_{-q} \rangle$ vanishes for small q , as $S_q \sim |q|^\alpha$ with $\alpha > 0$. HU is observed in numerous systems [2,3], ranging from sandpile models [4–9], and sheared colloids [10], to densest packings [11]. All the above systems have a critical state recognized to be in the conserved directed percolation (CDP) class. This attribution usually relies on a comparison of numerically measured critical exponents, especially the hyperuniformity exponent α . In this situation it is highly desirable to have an analytical understanding of the underlying mechanism for hyperuniformity, and to know the relevant critical exponents with precision. In this Letter, we provide an exact mapping from CDP to depinning of an elastic manifold [12]. This mapping allows us to express the hyperuniformity exponent α in terms of the dimension d and the roughness exponent ζ at depinning,

$$\alpha = 4 - d - 2\zeta. \quad (1)$$

Using ζ from depinning gives α with higher precision than in most sandpile simulations; see Fig. 1.

This Letter is organized as follows: We first review the concept of hyperuniformity, before introducing the Manna sandpile, the simplest and most prominent model in the CDP class. We then discuss further models in this class, and present the mapping. We finish with numerical evidence, and a discussion of relevant work in the literature.

Hyperuniformity—Consider a particle system of size L , where the total number N_{tot} of particles is conserved.

We ask how many particles N_R are in a part of the system of radius $R \ll L$. If the system is translationally invariant, then

$$\langle N_R \rangle = \frac{N_{\text{tot}}}{L^d} R^d. \quad (2)$$

How does N_R fluctuate? We expect that

$$\text{var}(N_R) = \langle N_R^2 \rangle - \langle N_R \rangle^2 \sim R^\kappa. \quad (3)$$

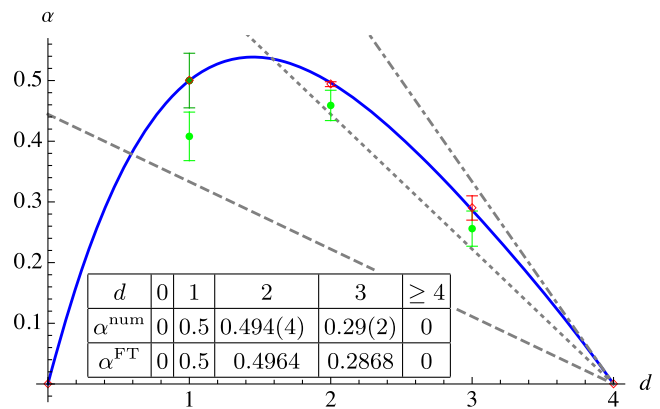


FIG. 1. The exponent α of the structure factor $S(q) \sim |q|^\alpha$ as a function of dimension d for the Manna model. The blue solid line is from the ϵ -expansion of [13], the red dots (with error bars) from simulations at depinning [14,15]. Simulations in green are from [16]. The dark green data point is from Fig. 2. In gray are the different ϵ -expansion results, $\alpha = c/9$ (dashed) [5], $\alpha = 2c/9$ (dotted) [17], and $\alpha = c/3$ (dot-dashed) [leading term of Eq. (25)].

One can show [18] that (except for fine-tuned models [19])

$$d - 1 \leq \kappa \leq d. \quad (4)$$

A Poisson process has $\kappa = d$, a regular lattice $\kappa = d - 1$. When $\kappa < d$ the system is said to be *hyperuniform*. This terminology was introduced in [1] for $\kappa = d - 1$, and is now used for any $\kappa < d$ [8,20,21]. Alternatively, one can consider the structure factor of the Fourier transform n_q of the density $n(x)$. Its small- q behavior is

$$S(q) = \langle n_q n_{-q} \rangle \sim q^\alpha, \quad \kappa + \alpha = d. \quad (5)$$

We are interested in class-III HU systems [2], which correspond to $0 < \alpha \leq 1$. Larger values of α are possible [2,22]; κ then freezes at its lower bound $\kappa = d - 1$.

The Manna sandpile and conserved directed percolation—The Manna sandpile [23] is defined as follows: Consider a d -dimensional lattice, e.g., the checker board in $d = 2$. Each site x has $n(x)$ grains. If $n(x) \geq 2$, with rate 1 move two of the grains, each to a randomly chosen neighbor. This dynamics conserves the total number $N := \sum_x n(x)$ of particles. Denote the fraction of i times occupied sites as a_i . Then (for each site x and time t) $\sum_{i=0}^{\infty} a_i = 1$, the number of particles is $\sum_{i=1}^{\infty} i a_i = n$, and the activity $\sum_{i=2}^{\infty} (i - 1) a_i = \rho$. The last definition, introduced in [24], gives a higher toppling rate to triple and higher occupied sites than the standard definition. Since we are interested in densities close to the transition, this does not matter [24]. The benefit of this definition is the existence of the exact sum rule,

$$n - \rho + e = 1, \quad (6)$$

where $e := a_0$ is the fraction of empty sites.

The next step is to write effective stochastic equations of motion for n , ρ , and e . Owing to the constraint (6) there are two independent equations, usually written in terms of particle density $n(x, t)$, and activity $\rho(x, t)$ (for a derivation see [24]),

$$\begin{aligned} \partial_t \rho(x, t) = & \nabla^2 \rho(x, t) + [2n(x, t) - 1]\rho(x, t) - 2\rho(x, t)^2 \\ & + \sqrt{2\rho(x, t)\eta(x, t)}, \end{aligned} \quad (7)$$

$$\partial_t n(x, t) = \nabla^2 \rho(x, t). \quad (8)$$

Here $\xi(x, t)$ is a standard white noise:

$$\langle \eta(x, t)\eta(x', t') \rangle = \delta^d(x - x')\delta(t - t'). \quad (9)$$

Sheared colloids—The same effective model works for periodically sheared colloids close to the reversible-irreversible transition. The connection can be understood via the random organization (RO) model [10]: Track the particle displacements after a full shear cycle of given

amplitude. These displacements are replaced by random ones of observed amplitude, for the active particles, i.e., those which collided during the cycle. This results again in the set of Eqs. (7) and (8). The biased random organization (BRO) model [11] is a variant, where colliding particles receive an additional displacement moving them apart. In [10,11] the authors claim that RO and BRO both belong to the CDP class. Furthermore, BRO is claimed to account for the statistics of random close packings (RCP) [11], where other authors claim RCP to be mean field in all dimensions [25].

Mapping CDP to depinning—We now map the CDP equations (7) and (8) onto depinning. Instead of writing coupled equations for $n(x, t)$ and $\rho(x, t)$, use the sum rule (6) to write coupled equations for $\rho(x, t)$ and $e(x, t)$,

$$\partial_t e(x, t) = [1 - 2e(x, t)]\rho(x, t) + \sqrt{2\rho(x, t)\eta(x, t)}, \quad (10)$$

$$\partial_t \rho(x, t) = \nabla^2 \rho(x, t) + \partial_t e(x, t). \quad (11)$$

To show the equivalence to disordered elastic manifolds [26,27], define

$$\rho(x, t) = \partial_t u(x, t) \quad (\text{the velocity of the interface}), \quad (12)$$

$$e(x, t) = \mathcal{F}(x, t) \quad (\text{the force acting on it}). \quad (13)$$

Equation (11) is the time derivative of the equation of motion of an interface, subject to a random force $\mathcal{F}(x, t)$,

$$\partial_t u(x, t) = \nabla^2 u(x, t) + \mathcal{F}(x, t). \quad (14)$$

It remains to characterize the statistics of \mathcal{F} . Since $\rho(x, t)$ is positive for each x , $u(x, t)$ is monotonously increasing. Instead of parametrizing $\mathcal{F}(x, t)$ by space x and time t , it can be written as a function of space x and *interface position* $u(x, t)$. Setting $\mathcal{F}(x, t) \rightarrow F(x, u(x, t))$, Eq. (10) becomes

$$\begin{aligned} \partial_t \mathcal{F}(x, t) & \rightarrow \partial_t F(x, u(x, t)) \\ & = \partial_u F(x, u(x, t))\partial_t u(x, t) \\ & = [1 - 2F(x, u(x, t))]\partial_t u(x, t) \\ & \quad + \sqrt{2\partial_u F(x, u(x, t))\eta(x, t)}. \end{aligned} \quad (15)$$

For each x , this is equivalent to an Ornstein-Uhlenbeck [28] process $F(x, u)$, defined by

$$\partial_u F(x, u) = 1 - 2F(x, u) + \sqrt{2}\xi(x, u), \quad (16)$$

$$\langle \xi(x, u)\xi(x', u') \rangle = \delta^d(x - x')\delta(u - u'). \quad (17)$$

While the noise $\eta(x, t)$ is uncorrelated in time, $\xi(x, u)$ is uncorrelated in the interface position u . Given x , $F(x, u)$ is

a Gaussian Markovian process with mean $\langle F(x, u) \rangle = 1/2$, and variance in the steady state of

$$\left\langle \left[F(x, u) - \frac{1}{2} \right] \left[F(x', u') - \frac{1}{2} \right] \right\rangle = \frac{1}{2} \delta^d(x - x') e^{-2|u - u'|}. \quad (18)$$

Writing the equation of motion (14) as

$$\partial_t u(x, t) = \nabla^2 u(x, t) + F(x, u(x, t)), \quad (19)$$

it is the equation of motion of an interface with *position* $u(x, t)$, subject to a *quenched disorder force* $F(x, u(x, t))$. The latter is δ correlated in the x direction, and short ranged correlated in the u direction: it is a disordered elastic manifold subject to random-field disorder. As a consequence, the results for disordered elastic manifolds can be used for CDP and the Manna model.

Hyperuniformity in the Manna model—The roughness exponent ζ for the random manifold is defined via

$$\langle [u(x, t) - u(y, t)]^2 \rangle \sim |x - y|^{2\zeta}. \quad (20)$$

Equation (12) implies that ρ is not HU,

$$\langle \rho(x, t) \rho(y, t) \rangle^c \sim |x - y|^{2(\zeta - z)}, \quad (21)$$

where z is the dynamical critical exponent [12]. As a new result, let us calculate the particle-density correlation function. We have to identify $n(x, t)$ with the appropriate random-manifold field. Using Eqs. (8) and (12), we find $\partial_t n(x, t) = \nabla^2 \partial_t u(x, t)$, or after integration over time

$$n(x, t) = \nabla^2 u(x, t) + n_0. \quad (22)$$

Here n_0 is the conserved mean density of particles, i.e., the conserved total number of particles divided by the volume. Taking the derivatives implied by Eq. (22) yields

$$\langle n(x, t) n(y, t) \rangle^c \sim |x - y|^{2\zeta - 4}. \quad (23)$$

In Fourier space this implies our result (1),

$$S_q := \langle n_q n_{-q} \rangle \sim |q|^\alpha, \quad \alpha = 4 - d - 2\zeta. \quad (24)$$

Denoting $\epsilon = 4 - d$, and using for ζ its ϵ expansion $\zeta = (\epsilon/3) + \zeta_2 \epsilon^2 + \zeta_3 \epsilon^3$, see [29,30] (two loop) and [13] (three loop), α becomes

$$\alpha = \epsilon - 2\zeta = \frac{\epsilon}{3} - 2\zeta_2 \epsilon^2 - 2\zeta_3 \epsilon^3 + \mathcal{O}(\epsilon^4) \quad (25)$$

$$\zeta_2 = 0.0477709715468230578\dots \quad (26)$$

$$\zeta_3 = -0.0683544(2). \quad (27)$$

To obtain predictions for α in the CDP class, we can use Eq. (25) via Padé-Borel resummation supplemented by the knowledge of $\zeta_{d=0} = 2$ [12], and $\zeta_{d=1} = 5/4$ [8,15]. This leads to

$$\alpha_{d=1}^{\text{FT}} = 1/2, \quad \alpha_{d=2}^{\text{FT}} = 0.4964, \quad \alpha_{d=3}^{\text{FT}} = 0.2868. \quad (28)$$

Alternatively, use the best simulation results $\zeta_{d=2} = 0.753 \pm 0.002$ [14] and $\zeta_{d=3} = 0.355 \pm 0.01$ [14], to find

$$\alpha_{d=2}^{\text{num}} = 0.494(4), \quad \alpha_{d=3}^{\text{num}} = 0.29(2). \quad (29)$$

As Fig. 1 shows, $0 \leq \alpha < 1$ in all dimensions, the signature given in Eqs. (4) and (5) for a class-III hyperuniform system. The figure compares ϵ -expansion, numerical simulations for α [16] in the Manna model (see below), and predictions using Eq. (24) with ζ from simulations at depinning.

Active state—When disordered elastic manifolds are driven at a finite velocity v , the force correlations become δ correlated in time [12], and act like a thermal noise, leading to a roughness exponent $\zeta_{\text{moving}} = (2 - d)/2$. This gives the hyperuniformity exponent in the active phase,

$$\alpha_{\text{active}} = 4 - d - 2\zeta_{\text{moving}} = 2. \quad (30)$$

This was observed in the active phase of the RO and Manna models with center of mass conservation [31], as well as in nonequilibrium hyperuniform fluids [22].

Stability of CDP, and relation to DP—There was a long debate whether the Manna model, or the corresponding CDP theory, are in the same universality class as disordered elastic manifolds or whether they belong to a different universality class, the directed-percolation (DP) class. This question was finally settled in [26] by the arguments presented above. To understand how robust CDP is, replace in Eq. (7) the term $[2n - 1]\rho \rightarrow \lambda[2n - 1]\rho$, while keeping n as a (possibly unobservable) variable. The limit of $\lambda \rightarrow 0$ corresponds to DP. This changes Eq. (16) for $F(x, u)$ to

$$\partial_u F(x, u) = \lambda[1 - 2F(x, u)] - 2(1 - \lambda)\rho + \sqrt{2}\xi(x, u). \quad (31)$$

Compared to Eq. (16), it has an additional noise proportional to ρ , with both a mean and a variance. We expect that for given x , as long as $\lambda > 0$, the process $F(x, u)$ remains short range correlated with a correlation length $\xi_F \approx 1/\lambda$. (This conclusion was reached via a different argument in [26].) While the correlation length ξ_F diverges for $\lambda \rightarrow \infty$, we expect the CDP class to be robust as long as $\lambda > 0$, i.e., as long as there is a conserved density n , and it appears via a term proportional to $n\rho$ in the equation for $\partial_t \rho$. It would be interesting to repeat simulations on sheared colloids [32], for which opposite conclusions were reached.

Improved numerical checks—There is some tension between simulation results $\alpha_{d=1}^{\text{Manna}} = 0.41(4)$ [16], the seemingly accepted value $\alpha_{d=1}^{\text{RO}} \approx 0.45$ [3,10,11], and our

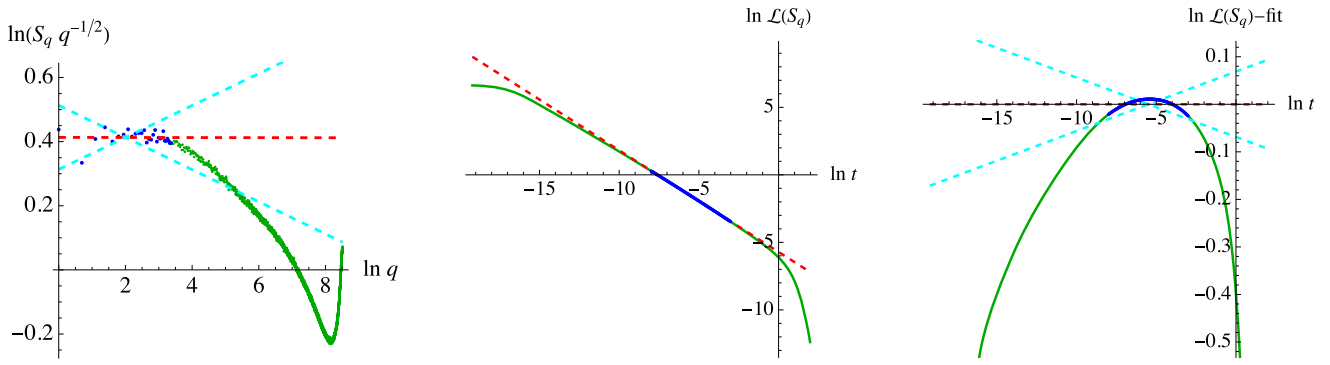


FIG. 2. Left: the compensated structure factor $S_q q^{-1/2}$ in a ln-ln plot for a periodic system of size $L = 10^5$, with 8×10^7 samples. The red dashed line with slope 0 indicates the behavior $S_q \sim \sqrt{q}$, and the cyan curves power laws with an exponent deviating by ± 0.05 , indicating our interval of confidence. The middle plot shows the Laplace-transform $\mathcal{L}_{\beta=1} \circ S(t)$ defined in Eq. (32). The fit by the red dashed line has slope $-(1 + \alpha) = -3/2$. Subtracting this fit gives the plot shown to the right.

exact result $\alpha_{d=1}^{\text{exact}} = 1/2$. For this reason we performed numerical simulations for Manna with systems of size up to $L = 10^4$. The results of the latter compensated for the predicted behavior are shown on the left of Fig. 2. There are strong finite-size corrections which make understandable the relatively small value given in [16]. However, in the relevant limit of small q , the data are consistent with $\alpha = 0.5$ (red dashed line), while the cyan (bright) lines for $\alpha = 0.45$ and $\alpha = 0.55$ are the confidence interval reported on Fig. 1. To reduce the statistical noise, we also show the results for a generalized Laplace transform,

$$\mathcal{L}_{\beta} \circ S(t) := \sum_q e^{-|q|^{\beta} t} S_q \sim t^{-\frac{1+\alpha}{\beta}}. \quad (32)$$

The value $\beta = 1$ is the standard Laplace transform, and was used, e.g., in [33]. $\beta = 2$ is now popular under the name “diffusion spreadability” [34]. Our data analysis shows $\beta = 1, 2$ or 4 to be equivalent for all practical purposes. As Fig. 2 for $\beta = 2$ reveals, the noise is indeed reduced, but it is more difficult to choose the proper domain to fit to. All fits give $\alpha = 0.5 \pm 0.05$.

The reader may wonder where this problem in such a large system comes from, and whether there might be systematic corrections. While there is no proper theoretical motivation, on a phenomenological level the deviations from a pure power law are well fitted with a logarithm, as Fig. 3 attests. To proceed, it is instructive to plot the density correlations as a function of distance. For short even distances, we find positive correlations, due to events where one grain is moved to the right, and one to the left. These positive correlations become negative for $x \geq 8$, but one has to wait to $x \approx 30$ until even and odd correlations are comparable. This indicates that $\ell = 30$ is the minimal coarse graining size, taking out 1.5 decades from the fitting range for S_q , certainly one reason for its slow convergence. One may also wonder whether this is related to the saturation of the apparent roughness exponent at depinning $\zeta_{\text{app}}^{\text{dep}}(d=1) \approx 1$ [12,35].

Relation to the literature—Our results contradict two works from the literature: the phenomenological observation $\alpha = \epsilon/9$ [5] [we supplemented [5] with $[\rho]_L = \zeta - z$ as implied by Eq. (21)] and $\alpha = 2\epsilon/9$ [17] obtained from RG within the Doi-Peliti approach. None of these works uses functional RG, which is crucial to account for the nontrivial structure present at two-loop [29,30] and three-loop [13] order at depinning. Reference [17] does this calculation in terms of active and passive particles in a two-species model. The density of the latter is a linear combination of fields used here, $n_p = a_1 \approx n - 2\rho$. Since $n - n_0 = \nabla^2 u$ and $\rho = \partial_t u$, the scaling dimensions of the two terms differ by $z - 2 = \mathcal{O}(\epsilon)$. As a result, n_p is not a proper scaling field of the RG, a problem known in other contexts [36]. As the two fields are degenerate at $\epsilon = 0$, their respective $\mathcal{O}(\epsilon)$ corrections are easily attributed to the $\mathcal{O}(\epsilon)$ correction of their linear combination n_p .

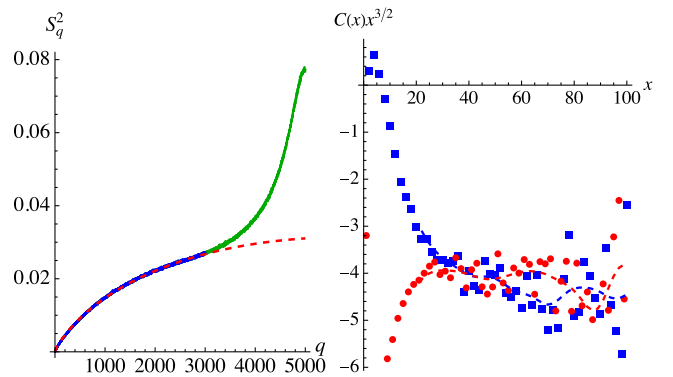


FIG. 3. Left: fit (red dashed) of S_q^2 (solid blue used for fit, green not used) for $L = 10^5$ with $S_q^2 \approx 5.31 \times 10^{-6} q \ln(16111/q)$. Right: The compensated correlation function $C(x)x^{3/2}$ for even (blue squares) and odd (red discs) distances x . In dashed weakly filtered data as guide for the eye. One sees strong even-odd lattice effects, which start to disappear at $x \approx 30$.

A new feature of [17] is the introduction of a current noise in their Eqs. (4) and (5). As additional terms have to vanish in the absorbing state $\rho = 0$, we may add to Eq. (10) the divergence of a current; the most relevant is $\nabla \vec{J}(x, t) \equiv \nabla \partial_t \vec{\Gamma}(x, t)$, with $\partial_t \vec{\Gamma}(x, t) = \sqrt{\rho(x, t)} \vec{\eta}(x, t)$, $\langle \eta^i(x, t) \eta^j(x', t') \rangle = \delta^d(x - x') \delta(t - t') \delta^{ij}$. Comparing $\nabla^2 \rho \sim L^{\zeta - z - 2}$ to $\nabla \sqrt{\rho(x, t)} \vec{\eta}(x, t) \sim L^{[(\zeta - z)/2] - 1 - [(d + z)/2]}$ we conclude that the latter is perturbatively irrelevant as long as $d + \zeta > 2$, which is satisfied for all $d > 0$. It may become relevant nonperturbatively: using the same techniques as in the derivation of Eq. (18), $\Gamma^i(x, t)$ has the statistics of a random walk, $\langle [\Gamma^i(x, t) - \Gamma^i(x, 0)]^2 \rangle \sim |u(x, t) - u(x, 0)|$. Using results of the Brownian-force model [12] one gets $\zeta = \zeta_{\text{BFM}} - 1 = 3 - d$. This would destroy HU in dimension $d = 1$, in contradiction to simulations. As the current in the Manna model should not keep an infinite-time memory as a random walk does, we propose to modify the equation for $\vec{\Gamma}$ to an Ornstein-Uhlenbeck process in u , as in Eqs. (10) and (16): $\partial_t \vec{\Gamma}(x, t) = \sqrt{\rho(x, t)} \vec{\eta}(x, t) - \kappa \rho(x, t) \vec{\Gamma}(x, t)$, $\kappa > 0$. This takes into account that if two particles jump onto the same neighbor, contributing to the current J , a toppling will take place there, resulting (possibly after iteration) in a countercurrent. $\Gamma^i(x, t)$ then has correlations as Eq. (18), and $\nabla \partial_t \vec{\Gamma}(x, t)$ is irrelevant. While the mapping from the CDP equations (7)–(9) to depinning is exact, the additional irrelevant current in Manna makes interfaces constructed as $u(x, t) := \sum_{\tau=0}^t \rho(x, \tau)$ microscopically rough. This can be seen in simulations.

Conclusions—In this Letter, we have shown how hyperuniformity in CDP is related to depinning. This equivalence yields precise theoretical predictions for the hyperuniformity exponent in all dimensions, both close to the transition, and in the active state. It would be interesting to extend these results to other universality classes, as qKPZ [14,37–39], and to see whether the fascinating phenomenology in plastic depinning [40] has an equivalence in sandpile models.

Acknowledgments—I thank Duyu Chen and Ran Ni for sharing their knowledge on hyperuniform systems, and X. Ma, J. Pausch, and M. E. Cates for stimulating discussions. This work was supported in part by Grant No. NSF PHY-2309135 to the KITP.

[1] S. Torquato and F. H. Stillinger, Local density fluctuations, hyperuniformity, and order metrics, *Phys. Rev. E* **68**, 041113 (2003).
 [2] S. Torquato, Hyperuniform states of matter, *Phys. Rep.* **745**, 1 (2018).
 [3] Yusheng Lei and Ran Ni, Non-equilibrium dynamic hyperuniform states, [arXiv:2405.12818](https://arxiv.org/abs/2405.12818).
 [4] M. Basu, U. Basu, S. Bondyopadhyay, P. Mohanty, and H. Hinrichsen, Fixed-energy sandpiles belong generically to directed percolation, *Phys. Rev. Lett.* **109**, 015702 (2012).

[5] D. Hexner and D. Levine, Hyperuniformity of critical absorbing states, *Phys. Rev. Lett.* **114**, 110602 (2015).
 [6] S. B. Lee, Universality class of the conserved Manna model in one dimension, *Phys. Rev. E* **89**, 060101(R) (2014).
 [7] R. Dickman and S. D. da Cunha, Particle-density fluctuations and universality in the conserved stochastic sandpile, *Phys. Rev. E* **92**, 020104(R) (2015).
 [8] P. Grassberger, D. Dhar, and P. K. Mohanty, Oslo model, hyperuniformity, and the quenched Edwards-Wilkinson model, *Phys. Rev. E* **94**, 042314 (2016).
 [9] R. Garcia-Millan, G. Pruessner, L. Pickering, and K. Christensen, Correlations and hyperuniformity in the avalanche size of the Oslo model, *Europhys. Lett.* **122**, 50003 (2018).
 [10] S. Wilken, R. E. Guerra, D. Levine, and P. M. Chaikin, Random close packing as a dynamical phase transition, *Phys. Rev. Lett.* **127**, 038002 (2021).
 [11] S. Wilken, A. Z. Guo, D. Levine, and P. M. Chaikin, Dynamical approach to the jamming problem, *Phys. Rev. Lett.* **131**, 238202 (2023).
 [12] K. J. Wiese, Theory and experiments for disordered elastic manifolds, depinning, avalanches, and sandpiles, *Rep. Prog. Phys.* **85**, 086502 (2022).
 [13] M. N. Semeikin and K. J. Wiese, Roughness and critical force for depinning at 3-loop order, *Phys. Rev. B* **109**, 134203 (2024).
 [14] A. Rosso, A. K. Hartmann, and W. Krauth, Depinning of elastic manifolds, *Phys. Rev. E* **67**, 021602 (2003).
 [15] A. Shapira and K. J. Wiese, Anchored advected interfaces, Oslo model, and roughness at depinning, *J. Stat. Mech.* (2023) 063202.
 [16] M. Henkel, H. Hinrichsen, and S. Lübeck, *Non-Equilibrium Phase Transitions* (Springer, Dordrecht, 2008).
 [17] X. Ma, J. Pausch, and M. E. Cates, Theory of hyperuniformity at the absorbing state transition, [arXiv:2310.17391](https://arxiv.org/abs/2310.17391).
 [18] J. Beck, Irregularities of distribution. I, *Acta Math.* **159**, 1 (1987).
 [19] J. Beck, Randomness in lattice point problems, *Discrete Math.* **229**, 29 (2001).
 [20] A. Donev, F. H. Stillinger, and S. Torquato, Unexpected density fluctuations in jammed disordered sphere packings, *Phys. Rev. Lett.* **95**, 090604 (2005).
 [21] C. E. Zachary and S. Torquato, Hyperuniformity in point patterns and two-phase random heterogeneous media, *J. Stat. Mech.* (2009) P12015.
 [22] Q.-L. Lei and R. Ni, Hydrodynamics of random-organizing hyperuniform fluids, *Proc. Natl. Acad. Sci. U.S.A.* **116**, 22983 (2019).
 [23] S. S. Manna, Two-state model of self-organized critical phenomena, *J. Phys. A* **24**, L363 (1991).
 [24] K. J. Wiese, Coherent-state path integral versus coarse-grained effective stochastic equation of motion: From reaction diffusion to stochastic sandpiles, *Phys. Rev. E* **93**, 042117 (2016).
 [25] P. Charbonneau, J. Kurchan, G. Parisi, P. Urbani, and F. Zamponi, Glass and jamming transitions: From exact results to finite-dimensional descriptions, *Annu. Rev. Condens. Matter Phys.* **8**, 265 (2017).

- [26] P. Le Doussal and K. J. Wiese, An exact mapping of the stochastic field theory for Manna sandpiles to interfaces in random media, *Phys. Rev. Lett.* **114**, 110601 (2015).
- [27] H.-K. Janssen and O. Stenull, Directed percolation with a conserved field and the depinning transition, *Phys. Rev. E* **94**, 042138 (2016).
- [28] G. E. Uhlenbeck and L. S. Ornstein, On the theory of the Brownian motion, *Phys. Rev.* **36**, 823 (1930).
- [29] P. Chauve, P. Le Doussal, and K. J. Wiese, Renormalization of pinned elastic systems: How does it work beyond one loop?, *Phys. Rev. Lett.* **86**, 1785 (2001).
- [30] P. Le Doussal, K. J. Wiese, and P. Chauve, 2-loop functional renormalization group analysis of the depinning transition, *Phys. Rev. B* **66**, 174201 (2002).
- [31] D. Hexner and D. Levine, Noise, diffusion, and hyperuniformity, *Phys. Rev. Lett.* **118**, 020601 (2017).
- [32] E. Tjhung and L. Berthier, Hyperuniform density fluctuations and diverging dynamic correlations in periodically driven colloidal suspensions, *Phys. Rev. Lett.* **114**, 148301 (2015).
- [33] A. Rosso, P. Le Doussal, and K. J. Wiese, Avalanche-size distribution at the depinning transition: A numerical test of the theory, *Phys. Rev. B* **80**, 144204 (2009).
- [34] S. Torquato, Diffusion spreadability as a probe of the microstructure of complex media across length scales, *Phys. Rev. E* **104**, 054102 (2021).
- [35] H. Leschhorn and L.-H. Tang, Comment on “Elastic string in a random potential,” *Phys. Rev. Lett.* **70**, 2973 (1993).
- [36] A. Kaviraj, S. Rychkov, and E. Trevisani, Parisi-Sourlas supersymmetry in random field models, *Phys. Rev. Lett.* **129**, 045701 (2022).
- [37] L.-H. Tang, M. Kardar, and D. Dhar, Driven depinning in anisotropic media, *Phys. Rev. Lett.* **74**, 920 (1995).
- [38] G. Mukerjee, J. Bonachela, M. Munoz, and K. J. Wiese, Depinning in the quenched Kardar-Parisi-Zhang class I: Mappings, simulations and algorithm, *Phys. Rev. E* **107**, 054136 (2023).
- [39] G. Mukerjee and K. J. Wiese, Depinning in the quenched Kardar-Parisi-Zhang class II: Field theory, *Phys. Rev. E* **107**, 054137 (2023).
- [40] C. Reichhardt and C. J. Olson Reichhardt, Depinning and nonequilibrium dynamic phases of particle assemblies driven over random and ordered substrates: A review, *Rep. Prog. Phys.* **80**, 026501 (2016).